Thermal And Mechanical Loading On A Fire Protection Shield Due To A Combustor Burn-Through

N.L. Messersmith and S.N.B. Murthy

Purdue University
West Lafayette, IN 47907
USA

AGARD
Propulsion and Energetics Panel
88th Symposium

AIRCRAFT FIRE SAFETY

14-18 October, 1996
Dresden, Germany

FSS001024R

Thermal And Mechanical Loading On A Fire Protection Shield Due To A Combustor Burn-Through

N.L. Messersmith and S.N.B. Murthy
Purdue University
West Lafayette, IN 47907
USA

1. SUMMARY

A combustor burn-through can give rise to an under-expanded, sonic or supersonic jet of gases and flames out of the combustor. The pressure and temperature in the jet may be as high as the highest values of pressure and temperature arising in the combustor. In order to protect the engine and aircraft components from exposure to the jet over a period of time, a fire shield is installed adjoining the combustor. The United States Federal Aviation Administration has issued an Advisory Circular 20-135 redefining the requirements on the fire protection shield, and the overall objective of the project was to establish the basis for a preliminary design of a test facility and testing procedure for such fire shield materials. The current study was devoted to the determination of the mechanical and thermal loads that arise on the shield due to the impact of hot, high pressure, high speed jets. The results obtained assist in the identification of some of the essential features required in a test facility, and the test plans and procedures.

2. INTRODUCTION

In flight gas turbine combustors, a crack or opening in the combustor wall, which may be due to local heating and material failure, and therefore, often referred to as a burn-through, causes the high pressure and temperature gases within the chamber to escape in the form of a jet. On impact, the jet can cause extremely high heat transfer (accompanied by severe mechanical loads) to the impacted surface, and become a cause for fire. Depending on the installation of the engine, the impaction and the resulting fire can extend to the nacelle and the pylon, and, in rare cases, even to the wing. The jet and the resulting fire may also spread downstream along the engine. In all cases the effects are primarily dependent on the characteristics of the jet, namely the jet composition, pressure, temperature, and geometry of the wall opening.

In the worst condition, the pressure and temperature of the jet may be equal to the highest values of those quantities arising in the combustor; thus, the pressure may be 20 - 40 atmospheres in current engines, and the temperature may approach the adiabatic flame temperature of Jet A fuel, under near stoichiometric conditions. The size of the jet, which depends at its origin on the size and geometry of the opening in the combustor wall, is another parameter of importance. In practice, the size of the opening may be expected to be quite small at the time of wall failure, and then grow to some maximum size with a shape different from that at the beginning. The jet invariably is sonic or supersonic, depending on the nature of the combustor casing failure and the resulting geometry of the opening. For example, if the wall material at the opening 'petals' outward due to the local pressure difference across it, then a supersonic flow results due to the divergence of the opening. In all cases, it can be expected that there is substantial under-expansion in the jet at its origin, and therefore, the jet undergoes further expansion during its development. However, when the jet faces a surface, the flowfield development itself is affected by the separation distance of the impacted surface from the jet origin.

The jet may, in general, be chemically reactive, and often contain unburned fuel that is gradually undergoing reaction during jet development and accompanying entrainment of air. On impingement, it is possible for chemical reactions to occur on the impacted surface, assisted by the surface heating that increases due to both the jet impact and also the jump in temperature from the plate shock formed ahead of the jet fluid stagnation region. In practice, a common approach to the problem is to contain the fire to the vicinity of its source by means of a fire shield surrounding the combustor region. Ideally the fire shield should be capable of withstanding the mechanical and thermal loads imposed on it by the jet over a specified period of time without undergoing a failure and thereby causing a spread of fire to other parts. The chief interest in the current paper is in the mechanical and thermal loading generated on the fire shield under different conditions, a parameter of primary importance in the design and testing of a fire shield. It is noted that the fire shield under discussion here is different from firewalls currently installed to containing engine fires, which are regulated by well established standards.

In this regard, the United States Federal Aviation Administration has issued an Advisory Circular 20-135 concerning powerplant installation and propulsion system component fire protection methods, standards, and criteria [1]. Related FAR sections are given in Appendix I of the AC to provide guidance on demonstrating compliance with the FAR. The original fire protection methods were developed in the 1950's and the requirements for the installation of fire protection walls were specified in FAR 25. The 1990 Advisory Circular deals with protection against a more intense flame than previously specified, the so called standard flame. The more intense flame corresponds to a fire condition within the engine, which burns through the engine case, causing a high pressure, high temperature gas jet to escape. The pressure and temperature under consideration are 350-550 psi (2.4 - 3.8 MPa) and 3000 - 3500 °F (1650 - 1930 °C), respectively, with the test jet nozzle size specified as one inch diameter (25.4 mm). The location of the fire shield during a test is given as the distance of the fire shield from the combustor case as installed in practice. The duration of

the exposure of the fire shield to the jet is also modified in the new advisory: the burn-through protection is required to withstand a minimum flame temperature of 3000 °F (1650 °C) at the impacted surface for a period of 3 minutes under peak pressure operation of the combustor. The specific emphasis on the temperature at the fire shield surface is due to the possible reduction in jet temperature over its traverse to the impacted surface. It is noted that the AC does not specify such other features as (a) the composition of the jet material, especially its content of unburned fuel or other chemically active substance, (b) the growth of the jet from a small to a large size as a function of time, and (c) the influence of a cross-flow, that may often be present in the region of jet flow or over the impacted plate. However, the AC also addresses other aspects of engine installation.

At this time, there are no standardized test facilities and specified test requirements for undertaking such tests with the new test conditions. A suitable facility must include (a) a high pressure, hot gas generator, (b) a structure for locating a part or a sample of the fire shield material with adequate strength and freedom from vibration and warping during jet impact, and (c) the required observational tools and rig safety devices. The test requirements must address in particular any conditions under which the magnitude and character of the mechanical and thermal loads become critically severe for the integrity of the fire shield.

It has been proposed by the FAA that a new test facility be developed, along with a test plan, so that fire shield materials and structures can be adequately tested and proved for satisfaction of the Advisory Circular. The design of a test facility and the establishment of standardized test plans and procedures is a complex task involving technical, safety, and other considerations, that require substantial technical effort, and considerable evolution before a fully operational facility and testing routine can become established.

As part of a project supported by the FAA through a grant to Purdue University, a three-phase plan was developed for addressing the preliminary design of a fire shield test facility and the development of associated test procedure: Phase I for the determination of the nature and types of mechanical and thermal loads that can arise during impact of high temperature, high pressure, high speed jets on a simple impingement plate; this includes the development of a suitable gas generator and a test installation; Phase 2 for addressing complexities in the loads due to variations in the shape and orientation of the impact plate, and due to the chemical state of the jet; and Phase 3 for the actual development of the test facility and evolution of acceptable test procedures. Presently, Phase 1 activity is completed.

3. BACKGROUND

It may be pointed out at the outset that the currently reported investigation does not address the following issues: (a) the circumstances and causes that lead to the occurrence of a combustor (and engine case) burn-through; (b) the problem of detection of the presence of a hot gas (or flame) jet in the vicinity of a combustor, or of overheating or a flame at the fire shield; and (c) the materials utilized in the design and manufacture of a fire shield, that can become ignited at the temperatures of interest (for example, columbium), or that may become too heavy in providing the required structural integrity (for example, combinations of titanium, stainless steel, and insulation such as refrasil). These are extremely important issues of great current interest. Thus the current paper is devoted solely to the experimental investigations on the jet impingement processes following combustor burn-through. Other engineering contexts in which high speed jet impingement is significant are in thrust reversers, vertical lift generation, rocket-assisted landing, stagnation flow on leading edges, heating and cooling schemes, and certain manufacturing processes.

The FAA undertook some early tests [2-5] on jet impingement caused by combustor burn-through. The main concerns in the test program were (a) the method of simulating the jet resulting from combustor burn-through while ensuring the temperature and heat flux at the impacted surface, (b) the thermal loading caused by the jet impact on a plate representing a test article such as a fire shield, and (c) the establishment of jet exposure time under different conditions for the occurrence of a burn-through on various shield materials. Several options were tested for generating the hot gas jet, and a can burner with a hole in the blocking plate was established as satisfactory for generating hot gas (or flame) jets of required characteristics. The loading generated by the jet at the impingement location on a plate was established by measurement of pressure and temperature at the plate when separated by various distances from the combustor opening, which was varied from 0.25 - 2.0 inches (6 - 50 mm) in different tests. Typical observed temperature and pressure data are presented in Table I and Figs. 1a and 1b respectively. The early work also included tests with flat plates located at different orientations with respect to the jet axis, and plates with curvature. The data from these tests pointed to a need for more extensive investigations, and also became the basis for the AC issued later.

A basic schematic of the jet impingement flow conditions and structure is provided in Fig. 2. As can be seen, the nature of the high speed jet impingement is complicated in several respects: the initial development of the under-expanded jet, the jet development in the region of interaction with the impingement surface, and the spread of the jet over the surface. Several regimes of flow can be identified corresponding to different jet conditions and plate locations, with some similarity in selected features (including distribution of loading) in each regime.

Aside from the work of Gardon and Coponpue [6], and more recently Fox et al. [7,8] and Lee et al. [9], high speed jet impingement heat transfer has not been examined in depth. However, there exists much more information regarding the dynamics of a jet and impingement flow field, including surface pressure loads. Both Donaldson and Snedeker [10] and Iwamoto [11] have found that scaling of the impingement characteristics with respect to free jet

characteristics can be helpful, particularly in regard to the influence of the location of the impingement plate in a region of jet expansion or compression. A number of studies by Hunt and coworkers [12-14] present the surface pressure distribution for a variety of impingement conditions, and Cobbald [15] has considered the surface pressure distribution due to very high pressure ratio jet conditions. In general, two regimes of flow have been observed: one in which the peak pressure arises at the geometric center of impingement, and the other in which a stagnation bubble appears above the plate, with the peak pressure occurring over a ring of finite radius around the center of impingement. The stagnation bubble is a region of trapped air that recirculates due to the annular slip line shear layer that helps to contain the bubble. Ginzburg et al [16] hypothesize that the slip line shear layer formed by the shock triple point of the plate shock and inner jet shock serves to separate the wall boundary layer and create the stagnation bubble region. The presence of a stagnation bubble is found to create a region of high pressure over a larger surface area than for typical stagnation point flow. At sufficiently high pressures, the wall jet displays a series of reflected shock waves. None of these studies, however, measured surface temperature in the presence of a stagnation bubble and do not, for example, indicate the formation of an annular region of peak temperature on the surface. These conditions also lead to expansions strong enough to accelerate the flow in the vicinity of the impingement point to supersonic Mach numbers in the wall jet, resulting in shock rings. These shock rings create regions of rapidly varying temperature and pressure along the radial direction over the plate, with potential for large gradients and associated stresses.

Recently, a number of computational studies of the supersonic jet impingement process have been published, see Tsuboi et al. [17], Kim and Chang [18-19], and Hong and Jeon [20]. The impinging flow presents a formidable challenge to CFD, with numerous shocks, shock-shock interactions, and shock-shear layer interactions; nevertheless, recent results are illuminating. Tsuboi et al. [17], Kim and Chang [18] have studied the three dimensional problem of inviscid jet impingement on an inclined plate, and compared predictions with the surface pressure measurements of Lamont and Hunt [13]. Furthermore, they indicate an interesting azimuthal pattern of fast and slow streams in the surface velocity vectors. While the simulation is inviscid, if the pattern is taken as representative of some plane near the wall boundary, the expectation would be to see associated variations in the surface temperature due to convection. Similar patterns have been observed by Yokobori et al. [21] in low speed jet impingement and have been attributed to localized enhancement of convective heat transfer due to the presence of streamwise vorticity in the developing region of the jet. Kim and Chang [19] have also considered the normal impingement of an inviscid, axisymmetric jet with nonequilibrium air properties. They demonstrate the possibility that variable thermal properties may have a significant influence on the structure of the jet flow, particularly in the flow region between the plate shock and the surface. Hong and Jeon [20] have developed a 3D Navier-Stokes solver for the case of jet impact on a flat plate, and this holds some promise for the future. It is noted here that in current practice, the ability of the fire shield to withstand the jet loads is often demonstrated through numerically predicted loads. However, calculations at less than the Navier-Stokes level can not be trusted to yield all of the complex loads and their distributions.

For high speed jet impingement heat transfer, the jet flow shock structure is important, and several recent works also indicate that unsteady flow processes can also arise and significantly alter the surface heat transfer characteristics. Fox et al. [7] considered a high subsonic jet (M=0.9) and proposed that a local separation of stagnation temperature occurs due to the unsteady pressure field associated with the passage of coherent vortex structures in the jet. This concept was called 'vortex-induced total temperature separation.' This is different from the 'shock-induced total temperature separation' mechanism under supersonic flow conditions recently proposed by Fox and Kurosaka [8] to explain observations of localized cooling in supersonic jet temperature distributions. The vortex-induced separation seems to explain both peaks and valleys in the radial distribution of total temperature in subsonic jets in both the near- and farfield. Goldstein et al. [22] suggested that the local cooling found in low speed jet impingement at small plate separation distances is the result of annular vortex ring-induced energy separation while Yokobori et al. [21] proposed streamwise vorticity. Meola et al. [23] have also recently found that large scale recirculations formed in the jet impingement process may explain the secondary peak in heat transfer coefficient observed in close impingement. Clearly, unsteady vortical motions can have a significant influence on impingement heat transfer; yet there is not a consensus on the underlying mechanism responsible for these effects. The current experimental results do indicate that it is possible under supersonic flow conditions to establish regions on the surface that are hotter or cooler than the jet stagnation temperature, which may be of significance in identifying specific jet impingement conditions for testing fire shields.

In summary, from the point of view of testing fire shield materials and structures, there are considerable ambiguities in regard to the following: a) the regimes or groups of conditions that characterize the changes in the impingement loading; b) the scaling of the flowfield features and the impingement loading as a function of the jet and impingement parameters; c) the influence of chemical reaction and burning in the jet and at the impacted plate, including catalytic effects on the surface; and d) the scaling of the impingement loading as a function of time during which there may be changes in jet initial conditions, size of the jet, and the nature of the impacted surface. The current paper addresses only the first two aspects, and the associated experimental studies.

4. EXPERIMENTAL FACILITIES

The research centered around two test rigs, one referred to as the Main Facility (MTF) and the other referred to as the Auxiliary Test Facility (ATF). The MTF had a wider range of operating conditions than the ATF, including vitiated or non-vitiated high temperature flow at high pressures. The ATF was smaller in size, but the facility has access to a more extensive array of flow diagnostics. Numerous measurements were made of surface pressure, temperature and heat flux on the impingement plate for a variety of jet conditions and plate separation distances in both rigs. Key parameters of the two test rigs are outlined in Table II, and described in further detail by Stuerman [24] and Love [25].

While both rigs could operate with either a sonic nozzle (convergent nozzle, M=1.0) or a supersonic nozzle (convergent-divergent nozzle, M=1.5), in the MTF the stagnation temperature of air in the low temperature regime of jet operation was raised by mixing cold air with combustion products from a gas-fed heater. For the high temperature regime, a dedicated high pressure combustor was utilized to provide the jet fluid. In the ATF, the air supply was heated to about 40 °C using strip heaters.

In the ATF, the low stagnation temperature allows advanced diagnostics to be used. These included dynamic response temperature sensitive fluorescent paints as well as schlieren and planar Mie scattering flow visualization techniques to study the jet shock and vortex structure. Flow visualization using laser sheet Mie scattering and schlieren photography is used in both a qualitative and quantitative manner. Schlieren photography and stagnation pressure measurements provide information regarding the mean jet shock structure and the jet potential core length. The vortex structure is thought to play a key roll in the observed surface temperature patterns and time resolved snapshots of the jet vortex structure were obtained using a pulse laser Mie scattering visualization. Surface temperature measurements were conducted using the temperature sensitive fluorescent paint EuTTA (Europium Thenoyltrifluoroacetonate). A video camera was used to record the fluorescent paint response over the desired impingement area. EuTTA has an inverse intensity response as a function of temperature, which when calibrated allows conversion of intensity images to surface temperature maps. Since the ATF impingement plate is water cooled, the surface temperature distribution is directly proportional to the local heat flux distribution. The spatial resolution of the technique was found to be very good, although dependent on the optical magnification and video camera array resolution. However, use of the paint does place a restriction on the maximum allowable jet temperature to about 50°C.

In the MTF rig, 60 type K thermocouples were embedded in the front surface, the plate thickness and on the back surface. Also, 14 surface pressure taps were arranged in a cross on the test plate. Schlieren pictures of the flowfield were obtained in most of the regimes of test operation.

5. TEST PLAN AND CONDITIONS

A considerable amount of diagnostic testing was carried out, initially and throughout the test program. A summary of the tests conducted is provided in Table III. A number of additional tests were carried out when it was felt that the flowfield or the impacted plate processes showed an interesting feature. In particular the ATF was used to study the jet structure in greater detail, with emphasis on the impingement shock structure relative to the shock structure of a free jet. These studies were confined to the near field of the jet, with the location of the impact plate within the jet potential core, or slightly beyond it. In some of the tests, the length of the jet potential core was also measured. Other cases that demanded more in-depth study included conditions leading to the formation of a stagnation bubble, as well as conditions that were observed to give rise to stagnation temperatures at the impingement surface apparently higher than the jet stagnation temperature, an unresolved issue to date as stated earlier.

6. RESULTS

The test results may be considered under three groups: 1) the mechanical pressure loads generated on the plate, 2) the thermal loads generated on the plate, in the axial and radial directions, and 3) the structure of the jet both in terms of initial jet development and also in terms of the jet shock structure in the vicinity of the impact plate.

6.1. Surface Pressure Measurements

The mechanical loading on the impact plate can be evaluated from the surface pressure distributions. Figure 3 shows a series of surface pressure distributions at different operating pressure ratios (Pr) from a supersonic nozzle. The transition between a stagnation point-type distribution (Pr=5.0 and 5.5 in Fig. 3) and a stagnation bubble-type distribution (Pr≥6) is clearly observed. Also, as the pressure ratio increases, radially varying pressure fields are established outside of the stagnation ring, indicating the likely presence of annular shocks. The occurrence of this variation seems to be most apparent for moderate pressure ratios, which also correspond to the appearance of the stagnation bubble flow. It might be expected that the mechanical loading of a jet from a supersonic nozzle would be greater than for a sonic nozzle at the same jet pressure ratio, due to the reduced shock losses in the supersonic jet. However, the influence of the impingement distance relative to the length of the jet shock cell (which is dependent on the jet Mach number) and the strength of the plate shock complicate the assessment of mechanical loading.

On an overall basis, the pressure distribution on the plate can be integrated to estimate the total force exerted on the plate by the jet as a function of the jet pressure ratio. The results are shown in Fig. 4 for the convergent nozzle case at three different distances, and in Fig. 5 for the convergent-divergent (CD) nozzle case at the same distances. The CD nozzle case shows a relatively self-similar loading of the plate as a function of pressure for impingement between three and eight jet diameters. This response is also quite similar to the farfield loading (z/d=8)

of the sonic nozzle. The deviation observed for close impingement occurs for nozzle pressure ratios known to generate Mach disks at the end of the first shock cell [26] and are seen to generate a stagnation bubble on the plate. (Mach disks are normal or near-normal shocks that form in various supersonic flows when oblique shocks cannot satisfy local pressure and flow turning boundary conditions.) It is believed that at these close impingement distances, the plate shock couples with the naturally occurring Mach disk of the first jet shock cell and leads to elevated pressures in the stagnation region. Since the CD nozzle flow weakens or eliminates the natural formation of a Mach disk for the same pressure ratios, no such coupling is clearly observed. With increased pressure ratio the shock cells enlarge and are expected to eventually couple a Mach disk to the plate.

Figure 6 shows the maximum pressure on the impingement surface versus the jet pressure ratio. The maximum plate pressure is expressed in dimensionless form as the maximum dynamic pressure recovered on the plate normalized by the dynamic pressure at the nozzle exit, $(P_{pmax} - P_e)/(P_{tj} - P_e)$, where P_e is the static pressure at the nozzle exit. This parameter gives some indication of the combination of plate shock strength and recovered pressure at the plate. At high pressure ratios, the plate shock is so strong that nearly the entire dynamic pressure available at the nozzle exit for recovery is lost, and the pressure load on the plate is smaller. At the very low pressure ratios, the plate shock is weakest, so that total pressure losses are minimal, and it is possible to recover most of the initial dynamic pressure on the surface, with correspondingly large pressure load on the plate. An interesting region occurs, for the convergent nozzle, in the pressure ratio range from 4 to 8 (coinciding with the observed increased loading of the plate seen in Fig. 4), where secondary peaks in the pressure recovery occur. The explicit relationship between the total loading on the plate and possible coupling of the jet shock cell with the plate shock is at present not fully understood and requires further study. However, for the combustor burn-through scenario, surface pressure gradients at these conditions are critical when coupled with thermal gradients in the same regions of the impact plate.

6.2. Surface Temperature Measurements

Surface temperature measurements from the MTF impact plate are shown in Figs. 7 and 8 for impingement from a sonic and supersonic nozzle, respectively. At close impingement, (Fig. 7), the temperature distribution for Pr=7.8 indicates that the peak temperatures occur not at the centerline, but at a radius of about one jet diameter, consistent with the surface pressure (Fig. 3) distribution that showed a stagnation bubble. The existence of the stagnation bubble at this condition is not as clearly indicated by the surface temperature as by the surface pressures, and this is due to the fact that the MTF impingement plate is designed to simulate the response of an actual fire shield, and does not have a controlled thermal boundary condition on the rear of the plate. Thus, the surface temperature distribution is smeared somewhat due to conduction in the plate and to non-uniform rear surface boundary conditions. These effects are primarily located at the central impingement region, so that while other conditions may actually indicate a stagnation bubble flow, the MTF surface temperature distributions are not the best indicators of their presence. Figures 7 and 8 show that increasing jet pressure ratio leads to increased plate temperatures, except for the central temperature reduction in the case of a stagnation bubble. Despite the central cooling provided by the recirculating flow in the stagnation bubble, the surface temperatures are elevated in the region outside the stagnation bubble. The freely variable temperature condition on the back side of the MTF plate leads to a concentration of heat in the center of the plate with radial outflow due to heat conduction to the lower temperature regions, and, along with the effects of flow processes such as annular shocks and elevated annular pressures for stagnation bubbles, the redistribution of heat results in a peak heat flux at about r/d=2 from the center of impingement. In addition, the combination of the thermal stresses at these radial locations may couple with the peak mechanical loads of a stagnation bubble flow to lead to a potentially critical condition for failure of a fire shield.

In the ATF, the use of dynamic response temperature sensitive fluorescent paints and a water bath-cooled impingement plate permit a better assessment of the direct influence of flow processes on the surface conditions. Since the response of EuTTA is inversely proportional to the local temperature, high temperature regions appear dark relative to low temperature regions. This is seen in the surface temperature images shown in Fig. 9. Both Fig. 9a and 9b, for Pr=4.5 and 6.0 respectively, correspond to the impingement of a supersonic nozzle at z/d=4. The flow for Pr=4.5 exhibits a stagnation point flow condition, while the Pr=6.0 flow indicates the formation of a stagnation bubble with two annular shock rings. Of note is the broader region of higher surface temperature (dark) for Pr=4.5. For Pr=6.0 the warm regions are confined to the stagnation bubble in the center of the plate and thin annular rings that are assumed to coincide with the reflection of oblique shocks off of the surface in the wall jet flow [12]. Fig. 10 is a compilation of a number of surface temperature data sets at z/d=8 and for pressure ratios from 2 to 6, all for a supersonic nozzle. Shown is the radial variation of the difference between the surface temperature and the ambient temperature normalized by the difference between the jet stagnation temperature and the ambient temperature, $(T_p - T_a)/(T_{tj} - T_a)$. The jet stagnation temperature was 40 °C, near the 'turn-off' temperature of the paint and the ambient temperature was nominally 15 °C. Pressure ratios from about 3.0 to 5.5 indicate higher peak temperatures than for other jet pressures. When the impingement surface is brought closer to the nozzle, z/d=4, the surface temperature distributions for pressure ratios from 3 to 6 all exhibit lower peak temperatures, as illustrated in Fig. 11. The traces for Pr=4.5 and Pr=6.0 in Fig. 11 correspond to the images shown in Fig. 9a and 9b, respectively. It is often easier to detect the incipient stagnation bubble development from the temperature traces rather than from the images directly, as is the case for Pr=6

above, although, in other cases where the bubble is well defined, the images generally suffice. The presence of annular rings in the temperature profiles typically coincide with the presence of a stagnation bubble; however, annular rings may also appear as precursors to the formation of a stagnation bubble. Similar features were observed in the surface pressure traces in Fig. 3.

6.3. Jet Structure

It is clear that the mechanical and thermal loads due to jet impingement are a function of jet pressure ratio, the type of nozzle (convergent or CD), and the separation distance between the jet exit and the impacted surface. Numerous length scales and time scales associated with these parameters can be developed. For instance, Love et al. [26] have compiled substantial data regarding the characteristic shock cell length scales for a number of nozzle Mach numbers and a wide range of pressure ratios, including the shock cell length, the centerline length for either a regular or Mach reflection, and the diameter of a Mach disk (when present). An additional length scale is the jet potential core length, which is an indicator of the transition of jet flow to the fully developed, farfield jet flow. In the current investigation, the basic character of the free jet shock structure and the jet potential core length were obtained from schlieren imaging. Also, centerline traces of the jet stagnation pressure were obtained with a traversing total pressure probe. Characteristic total pressure traces along the jet centerline are shown in Fig. 12 for several jet pressure ratios from a sonic nozzle. For the sonic nozzle, a jet pressure ratio greater than approximately 3.8 will lead to the formation of a Mach disk at the end of the first shock cell. This is noted by the extended low total pressure reading following the initial jet expansion. As the inner subsonic jet behind the Mach disk mixes with the outer supersonic jet flow, the total pressure rises and exhibits the characteristic shock cell structure until significant mixing with the ambient fluid reduces the jet total pressure. These plots can be used to obtain an estimate of the length of the potential core of the free jet and to examine what type of free jet flow condition would naturally exist at a given location of the impingement plate. Figure 12 also supports the impingement surface pressures shown in Fig. 6, where moderate range pressure ratio jets are seen to recover a significantly greater portion of the initial dynamic pressure than much higher pressure ratio jets.

The variations noted in Fig. 6 are related to the local position of the impingement plate relative to the jet shock structure. This is more clearly seen by considering the height of the plate shock above the surface as a function of both jet pressure ratio and impingement distance. The location of the plate shock was estimated using schlieren photography, as shown in Fig. 13a and 13b for jet impingement at z/d=4 and for Pr=4.5 and 6.0, respectively. These are the same conditions as for the surface temperature images in Fig. 9. Significant differences in the jet structure and the resultant surface flow in the near field of impingement can be seen in different cases. From a large set of video data, the location of the plate shock is estimated as the impingement distance is varied with a constant jet pressure ratio. Figure 14 shows these estimates for a Pr=4 sonic jet compared to the free jet shock structure, and Fig. 15 shows the same type of comparison for a Pr=6 jet. The plate shock location is seen to correlate well with the free jet shock structure. Higher jet pressure ratios create a stronger initial Mach disk, and as seen in Fig. 15, this can lead to an extended region where the shock is in a relatively constant location above the impact surface. In contrast, the shock location is seen to 'cycle' with the plate location in the weaker shock cell regions. This means that relative to the jet shock cell, the plate shock tends to get 'locked' into a favored position within the shock cell until it becomes unstable and 'hops' to the next cell. Such hops are readily visible when conducting experiments with the temperature sensitive paints and are often accompanied by significant changes in the surface temperature distribution.

7. DISCUSSION

Based on the background studies and the current investigation, three possible failure modes are hypothesized for a fire shield experiencing jet impingement from a combustor burn-through: 1) elevated surface temperatures exceeding the limits for the plate material, 2) steep gradients in the surface temperature leading to severe internal thermal stresses in the material, and 3) the potentially severe mechanical stresses in the material imposed by the pressure force of the impinging jet, in conjunction with reduced structural strength at high temperatures. Accordingly, experiments have been focused on determining jet conditions that produce those modes. In summary, no single condition has been found that produces a clearly worst case heat transfer scenario. However, various regimes of magnitude and distribution of thermal and mechanical loads have been identified that may be utilized in generating a test plan for proof testing a fire shield material.

In terms of the jet structure, a major finding for isothermal and slightly heated jets is the observation of peak surface temperatures consistently greater than the jet stagnation temperature when the impact plate was placed at a distance corresponding to 75% to 100% of the free jet potential core length, as shown in Fig. 16 for results from both sonic and supersonic nozzles. Those results implicitly include the influence of the jet Mach number and pressure ratio, since the potential core length of a given jet is dependent on these parameters. They suggest that, for any desired jet pressure ratio and Mach number, a placement of the impact plate near the tip of the jet potential core causes the highest possible surface temperatures to be generated. At distances corresponding to the end of the jet potential core, however, the temperature distributions are typically quite broad. At closer impingement distances, lower central temperatures are observed, and steep temperature gradients due to shock processes in the wall jet region begin to appear. A stagnation bubble type of flow, which generally forms at high jet pressure ratios, close impingement, or combinations of the two, was also found to produce steep temperature gradients along the wall; however, the peak surface temperatures were generally lower than for

stagnation point flow. As a general rule, higher jet pressure ratios create stagnation bubble flows and the steepest temperature gradients along the wall, and as the plate distance from the nozzle exit is increased, so too the minimum pressure ratio necessary for a stagnation bubble to form also increases.

It is important to note that consistent results have been obtained with the MTF large jet and the ATF small jet. This suggests that over the range of conditions studied here, the absolute size of the jet opening does not have a significant effect, but must be considered in conjunction with other relevant length scales of the jet impingement process.

8. CONCLUSIONS

Considering the testing of a fire shield for its strength and structural integrity in case of a fire, it has been shown that a well-controlled hot gas facility is a necessity, and a high pressure combustor burning aviation gas turbine fuel can be designed and set up to meet the need. The test facility itself should be designed such that the fire shield under test can be located in front of the facility combustor nozzle and subjected to a number of hot jet exposures at various distances. While the testing may only be carried out with a part of the fire shield, the test article size must be compatible with the nozzle size as well as the physical dimensions involved in the configuration. The edge conditions of the test article become particularly significant in the test facility.

Under such a set conditions, the mechanical and thermal loads imposed on the fire shield are of particular interest in the regimes identified in the current study. The jet impingement experiments suggest specific failure modes that include peak surface temperatures possibly exceeding the jet stagnation temperature, induced thermal stresses from steep, radial temperature gradients on the surface, mechanical stresses from the impact pressure loading, or combinations of the above. It is then of importance to ensure that the test plan includes all those jet conditions under which the loads and their gradients are high, and also display special features such as a ring-type, or a radially varying-type distribution.

A set of simple tests under arbitrarily fixed sets of jet geometry and operating conditions cannot be adequate to provide the required proof of reliability and safety. Recommended specific conditions for testing are:

A) ***Highest operating pressure ratio of combustor, with a jet to plate separation dictated by the installation distance.*** This condition will vary depending on engine size and compression ratio, but it is expected to generate a stagnation bubble, annular shock rings, and a reasonably high bubble temperature.

B) ***Moderate pressures ($4 \le Pr \le 8$) and moderate plate distances ($4 \le z/d \le 8$).*** This region encompasses the stagnation bubble formation conditions with high values of precursor pressures and temperatures and annular shock rings, and potentially severe coupling of axial and radial thermal stresses with annular pressure loading.

C) ***Moderate pressures ($3 \le Pr \le 8$) and plate distances roughly 75% of the jet potential core length.*** These conditions correspond to stagnation point flow and the maximum observed temperatures on the plate, with relatively high jet pressure ratios. These conditions may also be considered as precursors to the stagnation bubble formation, with a slightly lower pressure ratio and/or slightly longer plate distance. The potential core length varies with jet pressure ratio and nozzle design, but generally follows the trends in Fig. 12, where for Pr=3 the core length is about 5-7 z/d, increasing to 12-16 z/d for Pr=6.

Even considering this one aspect of the overall problem, much still needs to be understood and quantified, for example, on the effects of time-dependent growth of burn-through hole (although the time to enlarge the jet opening may be sufficiently short as to make the final jet size the most relevant), flame jet conditions with unburned fuel, and complex fire shield geometry and structure. Confidence in numerical prediction schemes will grow as data from such measurements accumulate and clarify the physical mechanisms.

9. ACKNOWLEDGMENTS

The authors acknowledge the support of the Federal Aviation Administration, under grant No. 92-G-0024 (Mr. J. Newcomb, the technical monitor), and the interest of Mr. C. Meshulam. Professor C. M. Ehresman was very helpful with facility design and operation.

10. REFERENCES

[1] 'Powerplant Installation and Propulsion System Component Fire Protection Test Methods, Standards and Criteria,' Advisory Circular, AC 20-135, Dept. of Trans., Federal Aviation Administration, 1990.

[2] Rust, T., 'Investigation of Jet Engine Combustion Chamber Burn-Through Fire,' FAA-RD-70-68, 1971.

[3] Hill, R., 'The Feasibility of Burner Can Burn-Through Thermal Detection,' FAA-RD-72-134, 1973.

[4] Hill, R., 'Jet Engine Burn-Through Flame Characteristics,' FAA-RD-74-19, 1974.

[5] Demaree, J.E., 'Reevaluation of Burner Characteristics for Fire Resistance Tests,' FAA-NA-76-43, 1977.

[6] Gardon, R. and Coponpue, J., 'Heat Transfer Between a Flat Plate and Jets of Air Impinging on It,' ASME 61-ht-53, 1961.

[7] Fox, M.D., Kurosaka, M., Hedges, L., and Hirano, K., 'The Influence of Vortical Structures On the Thermal Fields of Jets,' *JFM*, 255, pp. 447-472, 1993.

[8] Fox, M.D. and Kurosaka, M., 'Supersonic Cooling by Shock-Vortex Interaction,' *JFM*, 308, pp. 363-379, 1993.

[9] Lee, C., Chung, M.D., Lim, B.L., and Kang, S.K., 'Measurement of Heat Transfer From a Supersonic

Impinging Jet Onto an Inclined Flat Plate at 45 Degrees,' *J. Heat Transfer*, 113, pp. 769-772, 1991.

[10] Donaldson, C.D. and Snedeker, R.S., 'A Study of Free Jet Impingement. Part I: Mean Properties of Fee and Impinging Jets,' *JFM*, 45, pp. 281-319, 1971.

[11] Iwamoto, J., 'Impingement of Underexpanded Jets on a Flat Plate,' *J. Fluids Eng.*, 112, pp. 179-184, 1990.

[12] Carling, J.C. and Hunt, B.L., 'The Near Wall Jet of a Normally Impinging, Uniform Axisymmetric, Supersonic Jet,' *JFM*, 66, pp. 159-176, 1994.

[13] Lamont, P.J. and Hunt, B.L., 'The Impingement of Underexpanded, Axisymmetric Jets on Perpendicular and Inclined Flat Plates,' *JFM*, 100, pp. 471-511, 1980.

[14] Kalghatgi, G.T. and Hunt, B.L., 'The Occurrence of Stagnation Bubbles in Supersonic Jet Impingement Flows,' *Aero. Quart.*, 27, pp. 169-185, 1976.

[15] Cobbald, T.J., 'The Impingement of Underexpanded Axisymmetric Rocket Motor Exhausts and Cold Jets on Flat Plates,' *Aero. J.*, 96, pp. 27-28, 1992.

[16] Ginzburg, I.P., Semiletenko, B.G., Terpigorev, V.S., and Uskov, V.N., 'Some Singularities of Supersonic Underexpanded Jet Interaction with a Plane Obstacle,' *J. Eng. Phys.*, 19, pp. 1081-1084, 1970.

[17] Tsuboi, M., Hayashi, A.K., Fujiwara, T., Arashi, K., and Kodama, M., 'Numerical Simulation of a Supersonic Jet Impingement on a Ground,' *SAE Trans.*, Sect. 1, Pt. 2, pp. 2168-2180, 1991.

[18] Kim, K.H. and Chang, K.S., 'Three-dimensional Structure of a Supersonic Jet Impinging on an Inclined Plate' *J. Spacecrafts and Rockets*, 31, pp. 778-782, 1994.

[19] Kim, K.H. and Chang, K.S., 'Axisymmetric Impingement of a Hot Jet on a Flat Plate: Equilibrium Flow analysis of High Temperature Air,' *Shock Waves*, 4, pp. 155-162, 1994.

[20] Hong, S.K. and Jeon, H.J., 'Computational Study of Supersonic Jet Impingement on Flat and Complex Surfaces,' AIAA 94-2326, 25th Fluid Dynamics Conf., Colorado Springs, 1994.

[21] Yokobori, S., Kasagi, N., Hirata, M., Nakamaru, M., and Haramura, Y., 'Characteristic Behavior of Turbulence and Transport Phenomena at the Stagnation Region of an Axisymmetrical Impinging Jet,' *Turbulent Shear Flows II*, Imperial College, London, pp. 4.12-4.17, 1979.

[22] Goldstein, R.J., Behbahani, A.I. and Heppelmann, K.K., 'Streamwise Distribution of the Recovery Factor and the Local Heat Transfer Coefficient to an Impinging Circular Air Jet,' *Int. J. of Heat and Mass Transfer*, 29, pp. 1227-1235, 1986.

[23] Meola, C., de Luca, L. and Carlomagno, G.M., 'Influence of Shear Layer Dynamics on Impingement Heat Transfer,' *Exp. Thermal and Fluid Science*, 13, pp. 29-37, 1996.

[24] Stuerman, M.T., 'Surface Thermal Loading Imposed By a Sonic or Supersonic Impinging Jet,' Master's Thesis, Sch. of Aero. and Astro., Purdue Univ., West Lafayette, Indiana, 1994.

[25] Love, J.G., 'Scalability of Mechanical and Thermal Loads in Underexpanded Jet Impact,' Master's Thesis, Sch. of Aero. and Astro., Purdue Univ., West Lafayette, Indiana, 1995.

[26] Love, E.S., Grigsby, C.E., Lee, L.P., and Woodling, M.J., 'Experimental and Theoretical Studies of Axisymmetric Free Jets,' NASA TR R-6, 1959.

Table I. Observed and Estimated Temperatures. Taken From References [2-5]

Pressure Ratio	Hole Diameter [inches]	Flame Velocity at Exit [ft/s]	Estimated Flame Temperature [°F]	Distance for 2500 °F [inches]	Distance for 2000 °F [inches]
4.0	2.0	2890	3700		
	1.5	2890	3700		
	1.0	2890	3700	~8.0	~10.0
6.0	1.0	2930	3800	~9.0	~11.0
9.0	1.0	3000	4000	~11.0	~15.0
11.0	1.0	3040	4100	~15.0	
16.0				36-40	42-46
20.0				44-50	53-59
25.0				56-62	68-74

Table II. Key Features of the Main Test Facility and the Auxiliary Test Facility

Parameters	ATF	MTF	Notes
Pressure, MPa	0.15-0.83	0.50-2.07	
Temperature, °C	15-40	100-350 700-1500	heater in MTF combustor in MTF
Nozzle exit diameter, mm	6.35	25.4	
Impingement plate distance / nozzle diameter	0-100	3-30	
Nozzle Mach number	1.0-1.5	1.0-1.5	
Nozzle Reynolds number x 10^{-5}	0.23-6.40	4.5-8.5	

Table III. Experimental Conditions

Convergent Nozzle			Convergent-Divergent Nozzle		
Pressure Ratio	z/d	Tt/Ta	Pressure Ratio	z/d	Tt/Ta
2	3, 4, 6, 8	1, 1.6 - 1.7	3.5	2, 3, 4, 6, 8	1, 1.06, 1.2 - 1.9
2.5	3, 4, 6	1, 1.6 - 1.7	4.5	2, 3, 4, 6, 8	1, 1.06, 1.2 - 2
3.5	3, 4, 6, 8	1, 1.8 - 2	4, 5	2, 3, 4, 6, 8	1, 1.06
4.5	3, 4, 6, 8	1, 1.8 - 2	2, 2.5, 3, 5.5, 6	3, 4, 6, 8	1, 1.06
3, 4, 5, 5.5	3, 4, 6	1	7.8	3, 6, 8	1, 1.1 - 2
7.8	3, 8	1.9	10, 12, 14, 16	3, 8	1

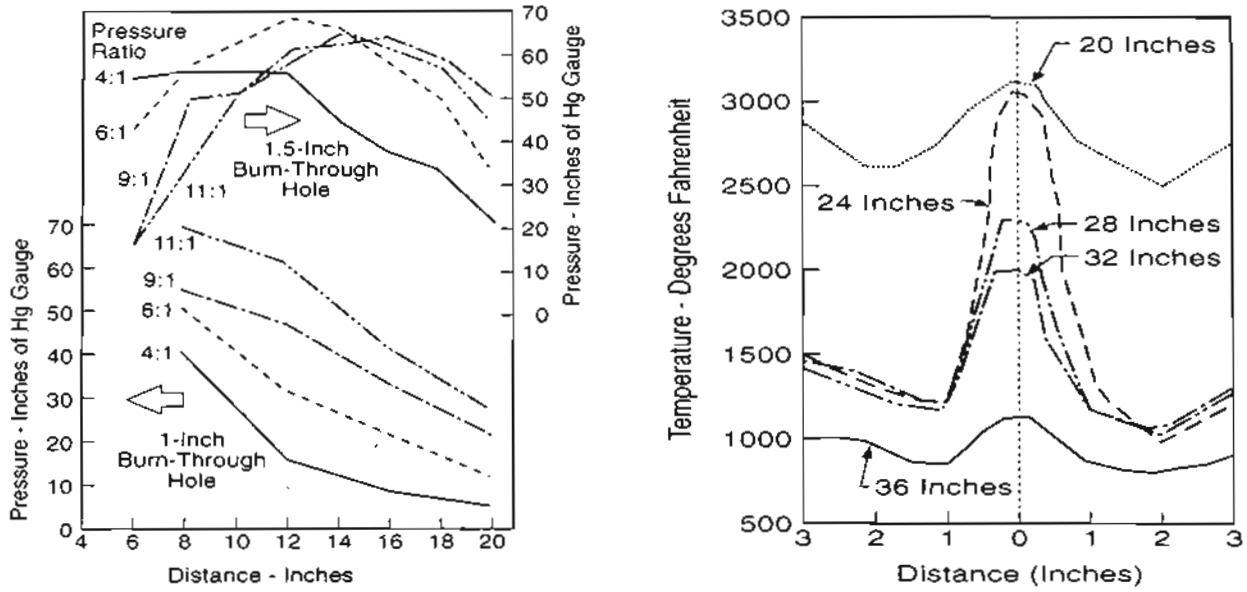

Figure 1. Results From Earlier FAA Studies of Hot Jet Impingement; a) Surface Pressures and b) Surface Temperatures. Redrawn From References [2-5].

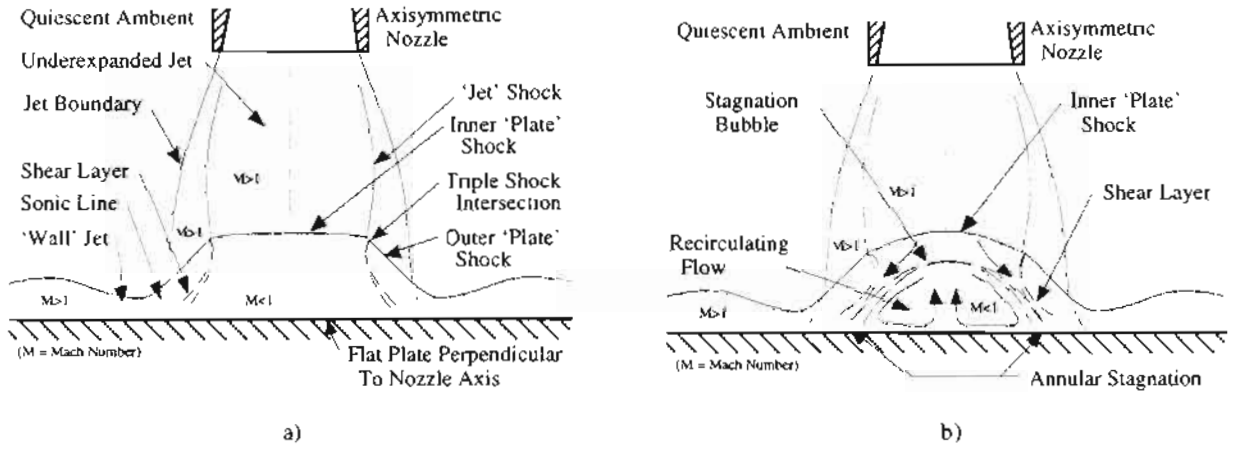

Figure 2. Schematic of Underexpanded Jet Impingement; a) Basic Gas Dynamic Flowfield and b) Stagnation Bubble Flowfield.

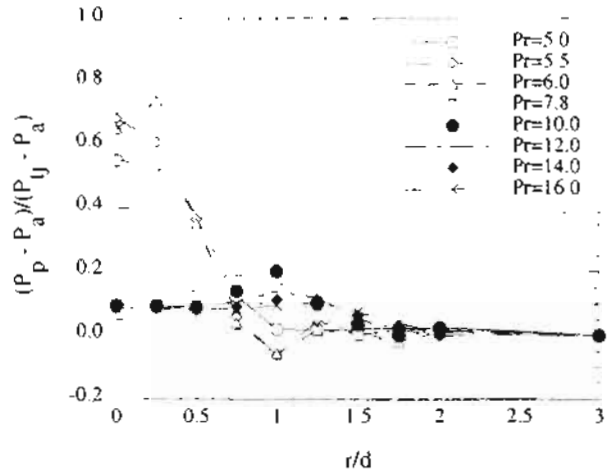

Figure 3. Radial Variation of Impingement Surface Pressure for Various Jet Pressure Ratios From a Supersonic Nozzle.

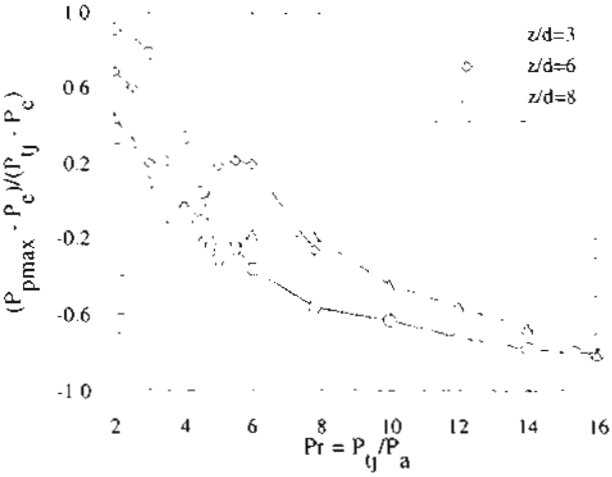

Figure 6. Recovery of Jet Dynamic Pressure at Impact Plate as a Function of Pressure Ratio and Impingement Distance.

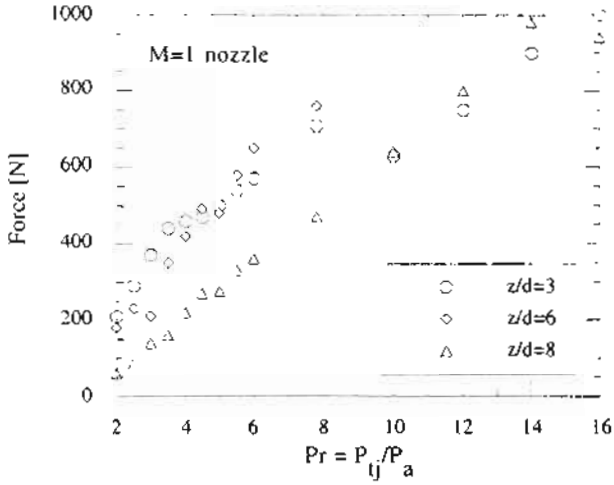

Figure 4. Integrated Force on Impact Plate From Sonic Nozzle as a Function of Distance.

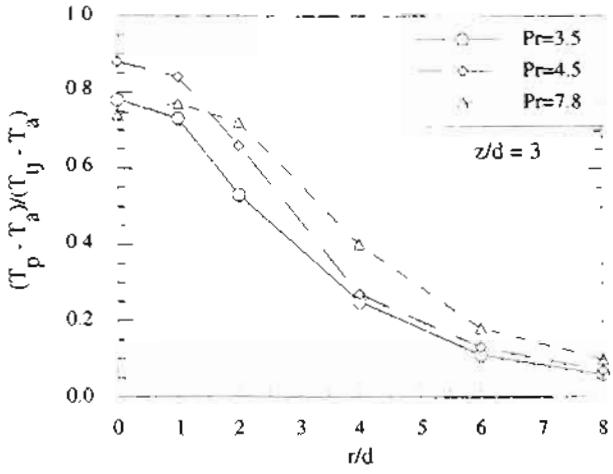

Figure 7. Radial Variation of Dimensionless Surface Temperature for Different Jet Pressure Ratios at z/d = 3.

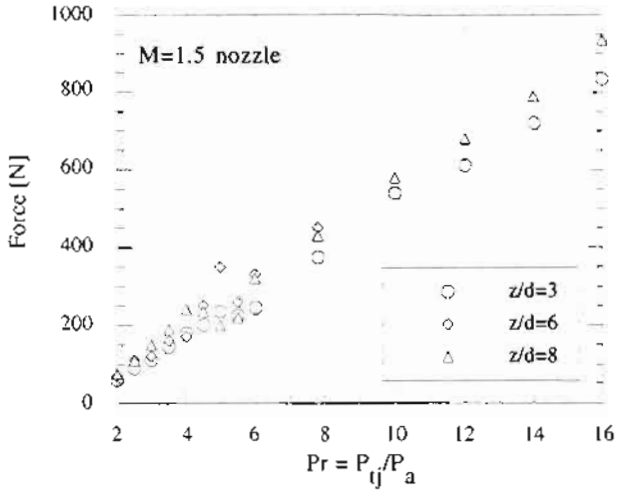

Figure 5. Integrated Force on Impact Plate From Supersonic Nozzle as a Function of Distance.

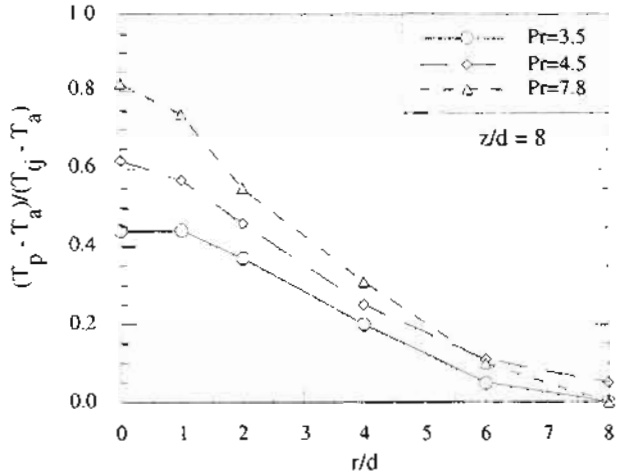

Figure 8. Radial Variation of Dimensionless Surface Temperature for Different Jet Pressure Ratios at z/d = 8.

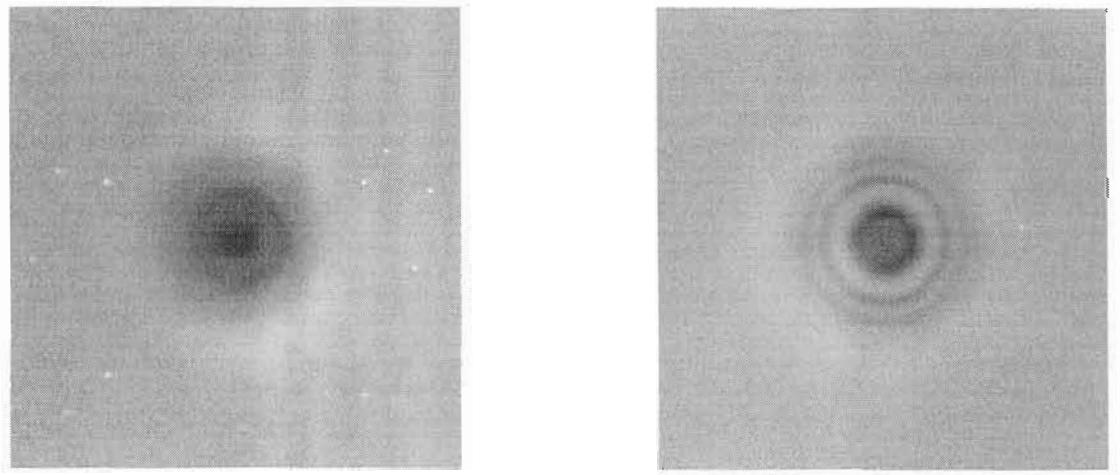

Figure 9. Jet Impingement Surface Temperature Images Using Temperature Sensitive Fluorescent Paint. Dark Regions Indicate Higher Temperatures Than Light Regions; a) Pr = 4.5 With a Stagnation Point Flow and b) Pr = 6.0 With a Stagnation Bubble Flow, Both For z/d = 4.

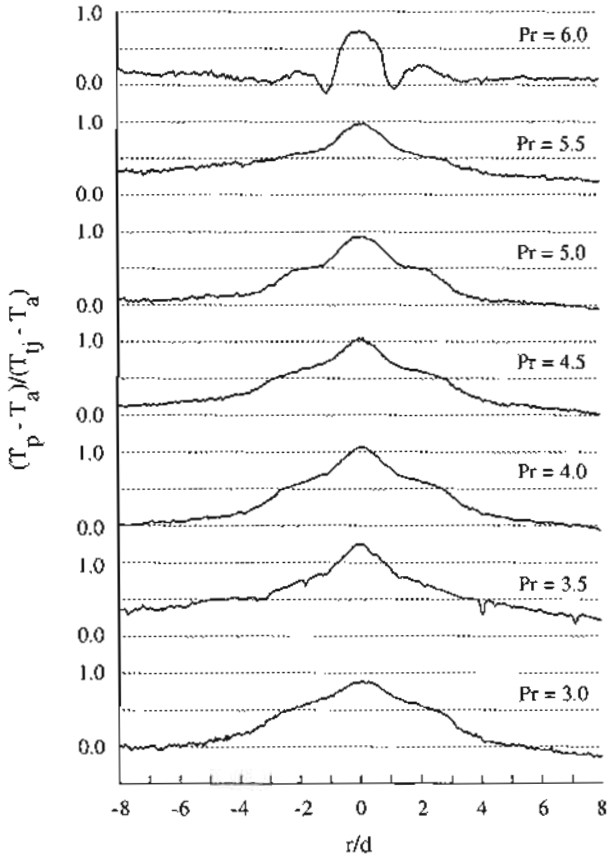

Figure 10. Radial Variation of Dimensionless Surface Temperatures for Different Jet Pressure Ratios Taken From Temperature Sensitive Fluorescent Paint. Mach = 1.5 Nozzle and z/d = 8.

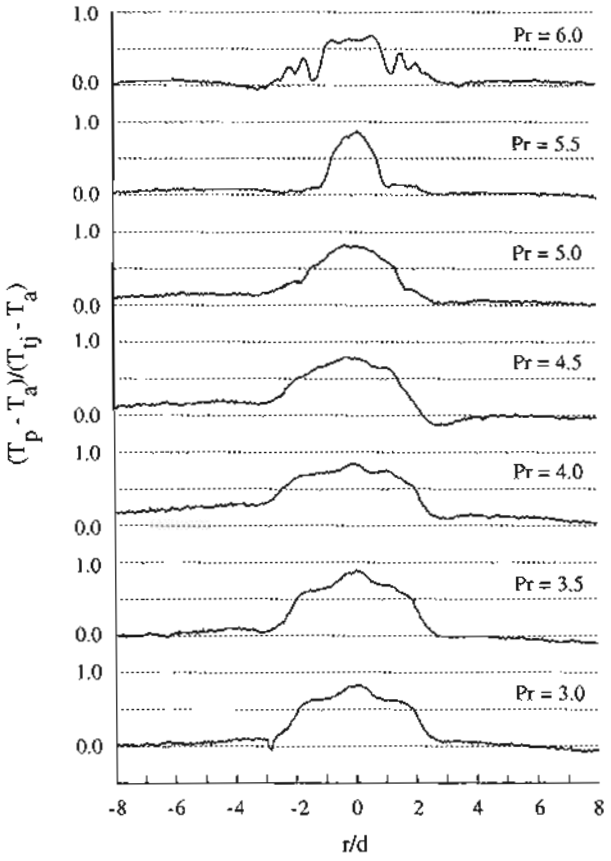

Figure 11. Radial Variation of Dimensionless Surface Temperatures for Different Jet Pressure Ratios Taken From Temperature Sensitive Fluorescent Paint. Mach = 1.5 Nozzle and z/d = 4.

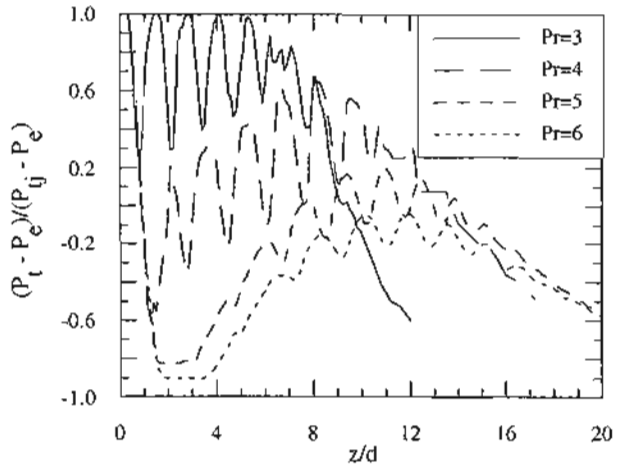

Figure 12. Free Jet Centerline Stagnation Pressure Profiles of Various Nozzle Pressure Ratios.

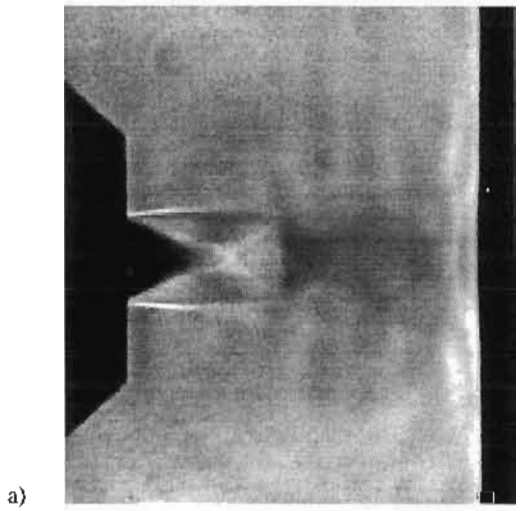

a)

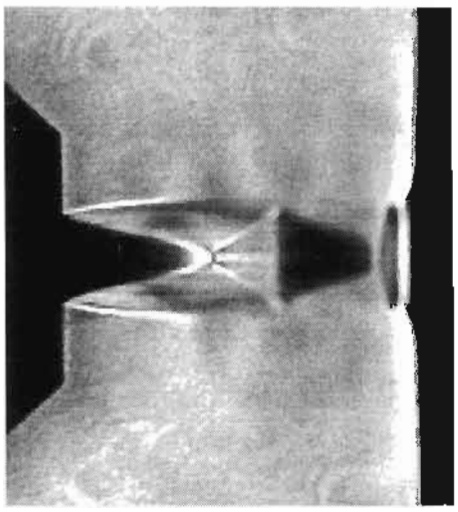

b)

Figure 13. Schlieren Images of Jet Structure in Impingement Region; a) Pr = 4.5 and b) Pr = 6.0, Both For z/d = 4. Conditions are the Same as for Figure 9a) and b).

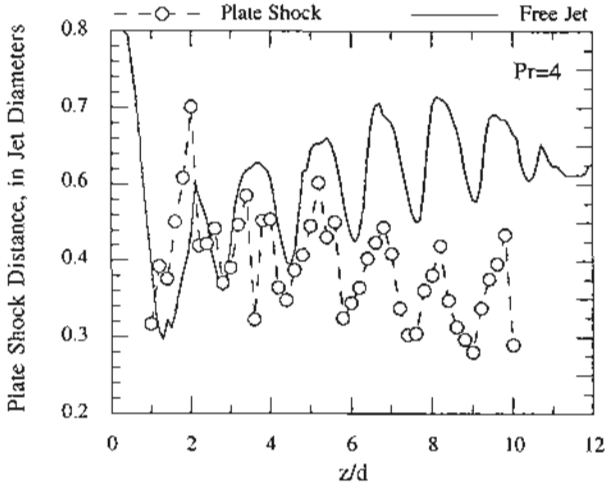

Figure 14. Plate Shock Distance Above Impact Plate to the as a Function of Plate Distance to Nozzle, Pr = 4.

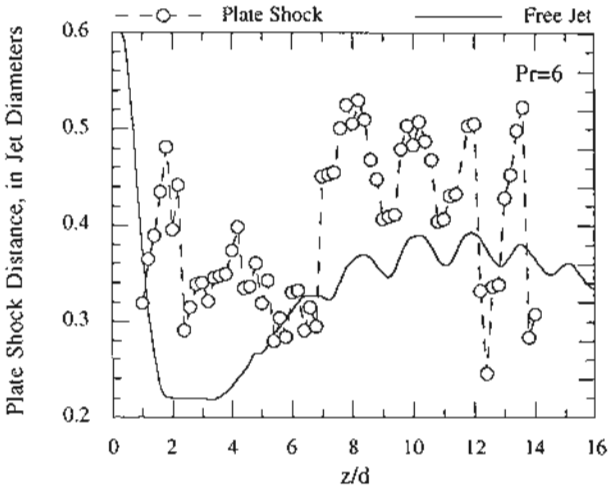

Figure 15. Plate Shock Distance Above Impact Plate to the as a Function of Plate Distance to Nozzle, Pr = 6.

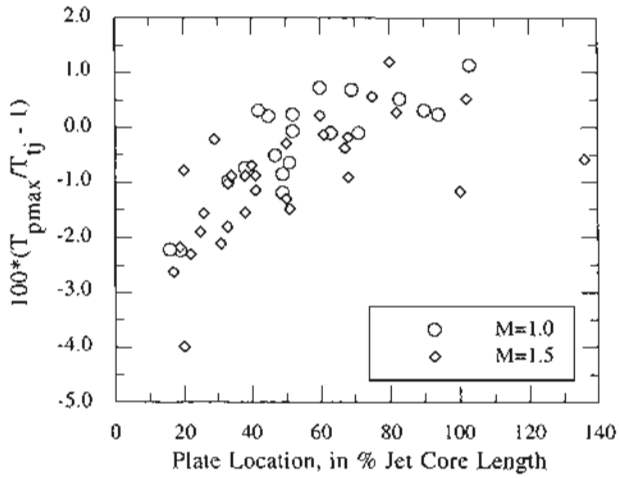

Figure 16. Peak Plate Temperatures as a Function of Plate Location with the Jet Potential Core.